Advances to the Blackstart and Fault Ride-Through Capability of Inverter-Based Resources (IBRs)

Hugo N. Villegas Pico
(✉ hvillega@iastate.edu)

Iowa State University (ISU)

PSERC Webinar
September 21, 2022

PSERC

Acknowledgements

Presentation based upon work funded by:
The U.S. Department of Energy, Office of Basic Energy Sciences
Office of Science Award #: SC0021410

Related publication for extended content and references:

H. N. Villegas Pico and Vahan Gevorgian, "Blackstart capability and survivability of wind turbines with fully rated converters," *IEEE Trans. Energy Conversion*, accepted for publication, 2022.

August 10, 2020 Derecho

Severe impacts to Midwest infrastructure (Iowa to Indiana): $7.5 billion
Blackout IA: around 600k customers without power

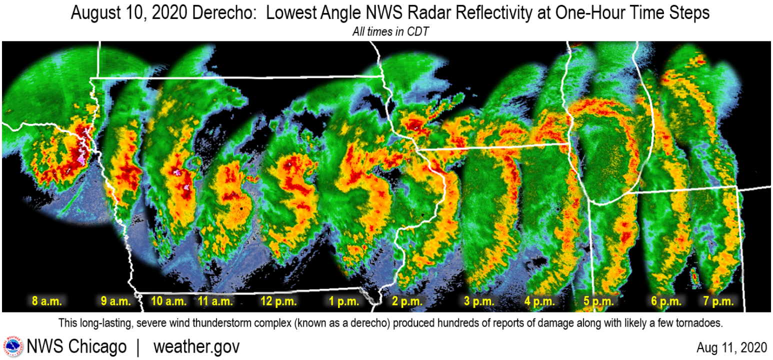

Other blackouts: South Australia (2016) and the United Kingdom (2019)

[1] K. Reynolds, "Request for Presidential Disaster Declaration," Office of the Governor, Aug. 16, 2020 https://governor.iowa.gov/sites/default/files/documents/Aug.%2010%2C%202020%20PresidentialDeclarationRequest.pdf

Wind Generation Capacity in the U.S.

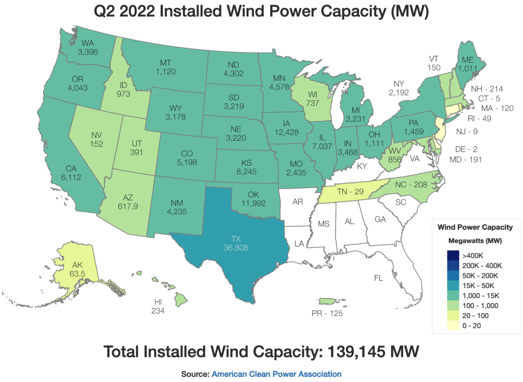

- Iowa 2022: 12.4 GW (wind)
- Iowa 2012: 5.13 GW (wind)

[1] https://windexchange.energy.gov/maps-data/321

[2] https://iub.iowa.gov/iowas-electric-profile

[1] https://www.ercot.com/files/docs/2022/02/08/ERCOT_Fact_Sheet.pdf

Wind-Dominant Power System

How do we restore a wind-dominant power system?

- blackstart and synchronize a group of wind turbines
- energize transmission, loads, and withstand faults

Problem: Present IBRs cannot participate in restoration

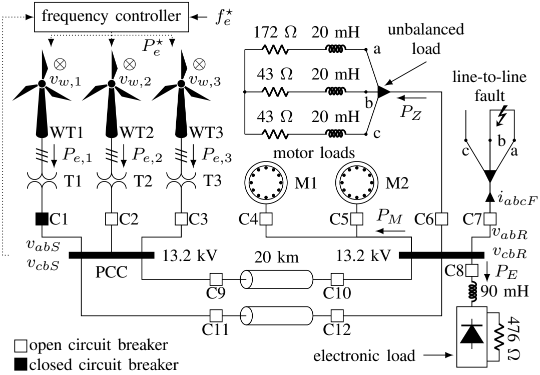

Significance of Addressing the Problem

- Satisfy NERC standard for recovery from blackouts: EOP-005-3 and EOP-006-3
- Meet NERC standard for frequency and voltage excursions: PRC-024-3
- Follow the recent standard IEEE 2800 for interconnection and interoperability of IBRs
- Address the third grand challenge in the science of wind energy: **System science for integration of wind power plants into the future electric grid**

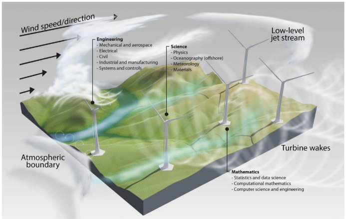

[1] P. Veers *et al.*, "Grand challenges in the science of wind energy" *Sci.*, vol. 336, no. 6464, pp. 1–9, Oct. 2019.

Type 4 Wind Energy Conversion Subsystem

Grid-forming operation

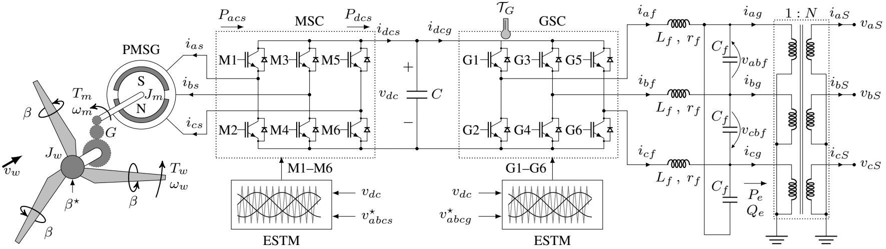

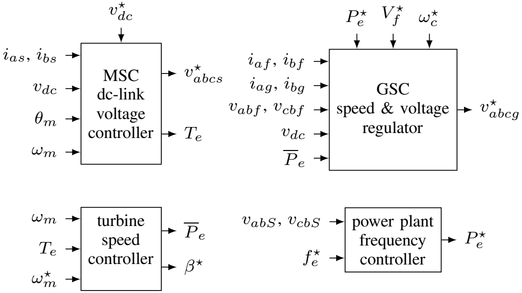

Specialty Transformations

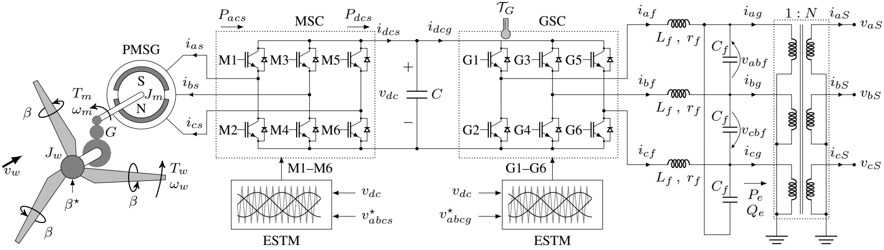

θ_c: angle of the GSC reference frame

$$abc \mapsto qd \text{ via } \theta_c$$

$$[v_{abf}\,, v_{cbf}]^\top \mapsto [v_{qf}^c\,, v_{df}^c]^\top = v_{qdf}^c$$

$$[i_{af}\,, i_{bf}]^\top \mapsto [i_{qf}^c\,, i_{df}^c]^\top = i_{qdf}^c$$

$$[i_{ag}\,, i_{bg}]^\top \mapsto [i_{qg}^c\,, i_{dg}^c]^\top = i_{qdg}^c$$

[1] P. C. Krause, O. Wasynczuk, S. D. Sudhoff, and S. Pekarek, *Analysis of Electric Machinery and Drive Systems*, 3rd ed. New York: IEEE Press, Wiley-Interscience, 2013

Type 4 Wind Energy Conversion Subsystem

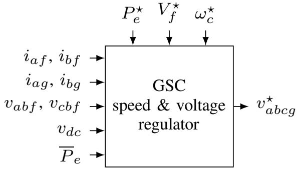

1. speed droop strategy (M. C. Chandorkar *et al.*, 1993)

$$\text{GSC reference frame speed: } \omega_c = \omega_c^* + \frac{\omega_b}{P_{e,\mathsf{mx}}} k_\omega (P_e^* - \widetilde{P}_e) - \omega_a \omega_b$$

$$\text{GSC reference frame angle: } \frac{d}{dt}\theta_c = \omega_c$$

$$\text{electric power: } P_e = \frac{3}{2}(v_{qf}^c i_{dg}^c + v_{df}^c i_{qg}^c)$$

2. *qd* voltage control for current-regulated converters (O. Wasynczuk *et al.*, 1996)
3. *qd*-axis anti-windup PI regulators that bound signals within a circle

Two-Axis Anti-Windup PI Regulators

Classical square bounding approach (anti-windup via conditional integration)

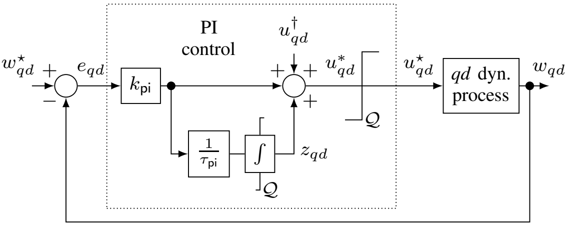

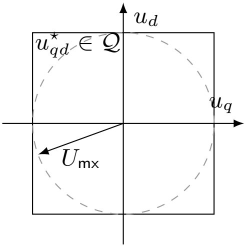

$$u_q^\star = \mathscr{L}(u_q^*, -U_{\mathsf{mx}}, U_{\mathsf{mx}})$$
$$u_d^\star = \mathscr{L}(u_d^*, -U_{\mathsf{mx}}, U_{\mathsf{mx}})$$
$$\mathscr{L}(\mu, \mu_{\mathsf{mn}}, \mu_{\mathsf{mx}}) = \begin{cases} \mu_{\mathsf{mx}} & \text{if } \mu > \mu_{\mathsf{mx}} \\ \mu_{\mathsf{mn}} & \text{if } \mu < \mu_{\mathsf{mn}} \\ \mu & \text{otherwise} \end{cases}$$

Two-Axis Anti-Windup PI Regulators

Circle bounding approach (anti-windup via series implementation)

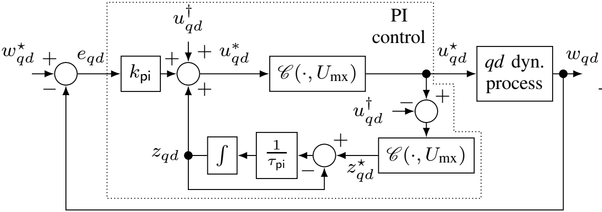

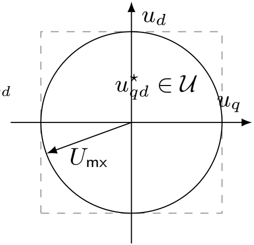

$\mathscr{C}$ bounds u^*_{qd} within an origin-centered circle, $\mathcal{U}$, of radius U_{mx}

$$\mathscr{C}(u^*_{qd}, U_{\text{mx}}) = \begin{cases} \frac{U_{\text{mx}}}{U} u^*_{qd} & \text{if } U > U_{\text{mx}} \neq 0 \\ u^*_{qd} & \text{otherwise} \end{cases}$$

$$U = \sqrt{u_q^{*2} + u_d^{*2}}$$

Two-Axis Anti-Windup PI Regulators

Classical two-axis PI regulators without anti-windups:

$$u_{qd}^{*} = k_{\mathsf{pi}}(w_{qd}^{\star} - w_{qd}) + z_{qd} + u_{qd}^{\dagger} \tag{1}$$

$$\frac{d}{dt}z_{qd} = \frac{k_{\mathsf{pi}}}{\tau_{\mathsf{pi}}}(w_{qd}^{\star} - w_{qd}) \tag{2}$$

Step 0: Recognize the obvious in (1):

$$k_{\mathsf{pi}}(w_{qd}^{\star} - w_{qd}) = u_{qd}^{*} - z_{qd} - u_{qd}^{\dagger} \tag{3}$$

Step 2: Redefine integrator dynamics by substituting (3) into (2):

$$u_{qd}^{*} = k_{\mathsf{pi}}(w_{qd}^{\star} - w_{qd}) + z_{qd} + u_{qd}^{\dagger} \tag{4}$$

$$\frac{d}{dt}z_{qd} = \frac{1}{\tau_{\mathsf{pi}}}(-z_{qd} + u_{qd}^{*} - u_{qd}^{\dagger}) \tag{5}$$

Two-Axis Anti-Windup PI Regulators

Step 3: Bound the control effort, u^*_{qd}, within a circle:

$$u^*_{qd} = k_{\mathsf{pi}}(w^\star_{qd} - w_{qd}) + z_{qd} + u^\dagger_{qd} \tag{6}$$

$$u^\star_{qd} = \mathscr{C}(u^*_{qd}, U_{\mathsf{mx}}) \tag{7}$$

$$\frac{d}{dt} z_{qd} = \frac{1}{\tau_{\mathsf{pi}}}(-z_{qd} + u^\star_{qd} - u^\dagger_{qd}) \tag{8}$$

Step 4: Bound the integrator commands, $u^\star_{qd} - u^\dagger_{qd}$, within a circle:

$$u^*_{qd} = k_{\mathsf{pi}}(w^\star_{qd} - w_{qd}) + z_{qd} + u^\dagger_{qd} \tag{9}$$

$$u^\star_{qd} = \mathscr{C}(u^*_{qd}, U_{\mathsf{mx}}) \tag{10}$$

$$z^\star_{qd} = \mathscr{C}(u^\star_{qd} - u^\dagger_{qd}, U_{\mathsf{mx}}) \tag{11}$$

$$\frac{d}{dt} z_{qd} = \frac{1}{\tau_{\mathsf{pi}}}(-z_{qd} + z^\star_{qd}) \tag{12}$$

Two-Axis Anti-Windup PI Regulators

Two-axis anti-windup PI regulators that bound control efforts and integrators within circles of radius U_{mx}

$$u^*_{qd} = k_{\mathsf{pi}}(w^\star_{qd} - w_{qd}) + z_{qd} + u^\dagger_{qd} \tag{13}$$

$$u^\star_{qd} = \mathscr{C}(u^*_{qd}, U_{\mathsf{mx}}) \tag{14}$$

$$z^\star_{qd} = \mathscr{C}(u^\star_{qd} - u^\dagger_{qd}, U_{\mathsf{mx}}) \tag{15}$$

$$\frac{d}{dt} z_{qd} = \frac{1}{\tau_{\mathsf{pi}}}(-z_{qd} + z^\star_{qd}) \tag{16}$$

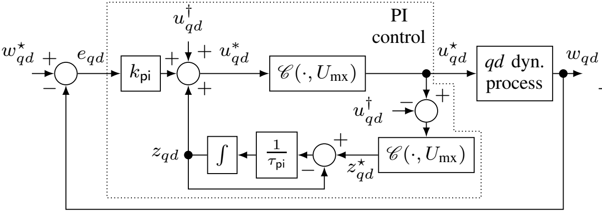

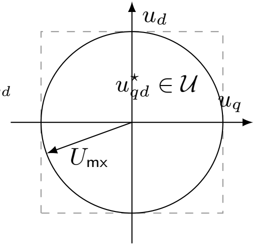

Blackstart + Restoration + Fault Ride-Through

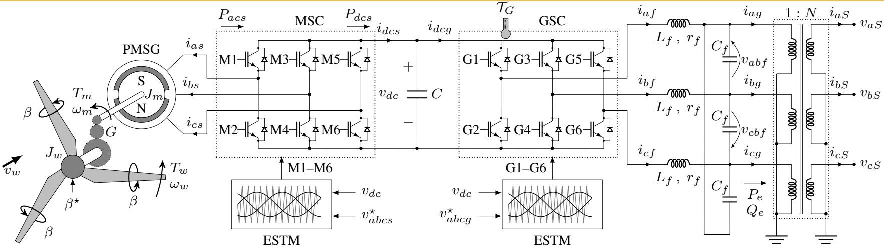

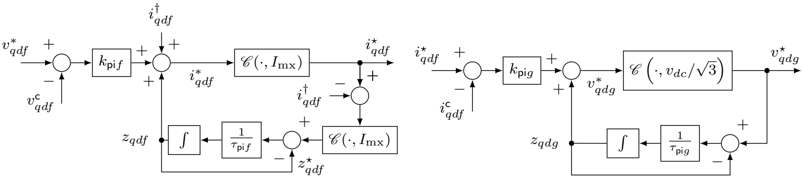

(a) Voltage regulator (b) Current regulator

feedforward currents: $$i^\dagger_{qdf} = 3C_f\omega_b v^c_{dqf} + i^c_{qdg} \qquad (17)$$

Simulation Results

Constructed a waveform-level simulation model in PLECS

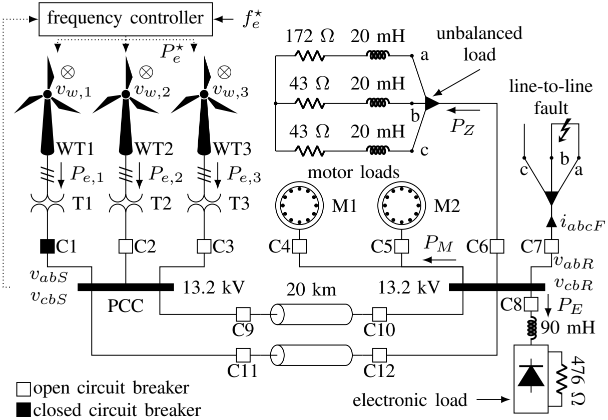

Circuit breaker times:

	C1	C2	C3	C9	C10	C4	C5	C11	C12	C6	C8	C7
close: t_c (s)	5.0	5.1	5.2	6.5	7.0	7.5	7.5	8.0	8.5	15	17.5	20.0
open: t_o (s)	-	-	-	-	-	-	-	-	-	-	-	20.5

Simulation Results

Startup $t = 2.5$ s, trans. cables $t \in \{6.5, 7, 8, 8.5\}$ s, motors $t = 7.5$ s, asym. load $t = 15$ s, electronic load $t = 17.5$ s, fault $t = 20$ s

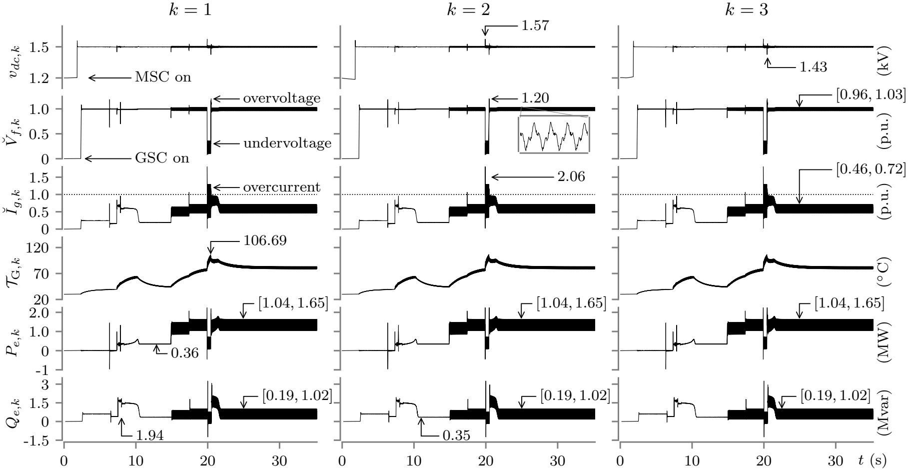

$$\breve{V}_{f,k} := V_{f,k}/V_b \text{ with } V_{f,k} := \sqrt{\left(v^c_{qf,k}\right)^2 + \left(v^c_{df,k}\right)^2} \tag{18}$$

Simulation Results

Waveforms during a 30-cycle line-to-line fault disturbance

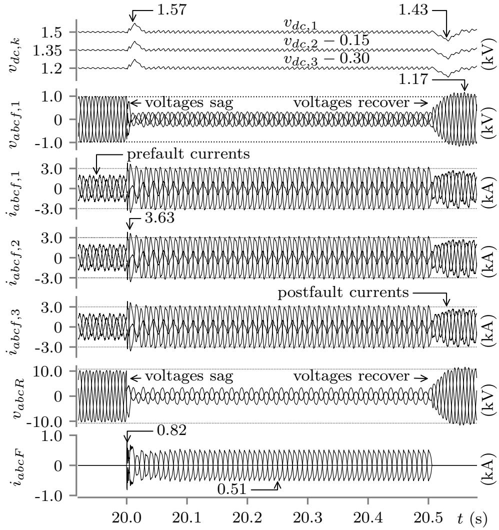

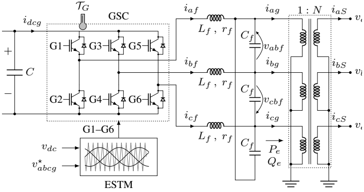

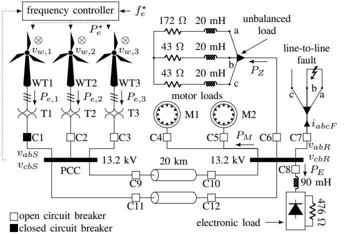

Simulation Results

Dynamic performance of loads during restoration and the line-to-line fault

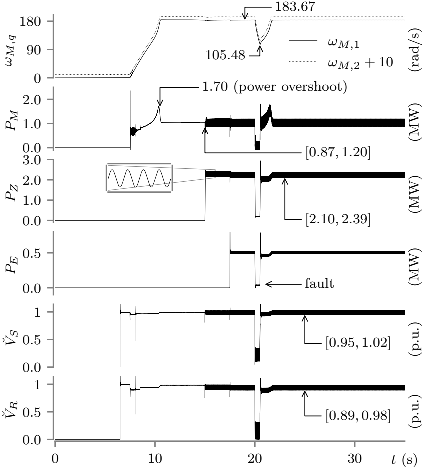

motors $t = 7.5$ s,
asym. load $t = 15$ s,
electronic load $t = 17.5$ s,
fault $t = 20$ s

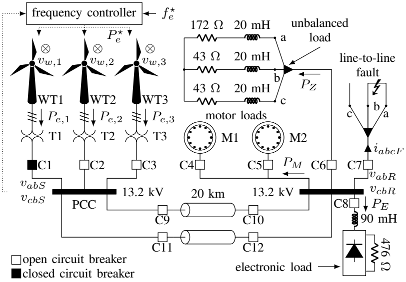

Simulation Results

Speed and frequency response during restoration

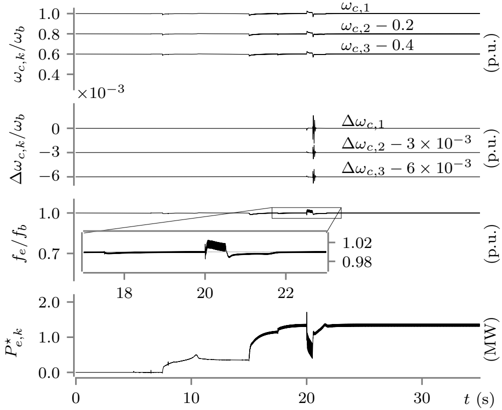

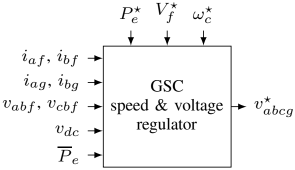

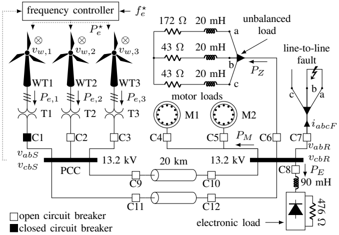

Relative speed:

$$\Delta\omega_{c,k} = \omega_{c,k} - (\omega_{c,1} - \omega_{c,2} - \omega_{c,3})/3$$

Implications: DFIG-Based Wind Turbines

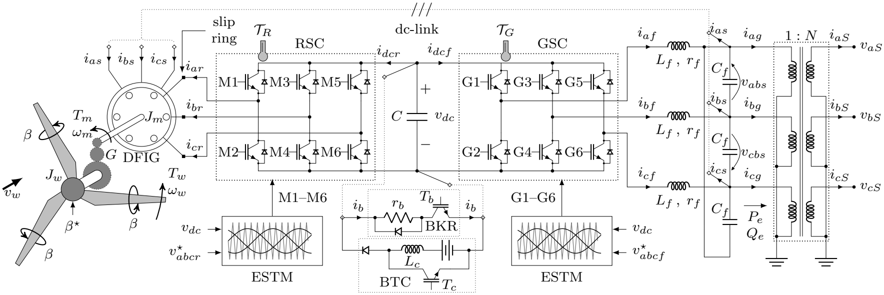

H. P. Dang and **H. N. Villegas Pico**, “Blackstart and fault ride-through capability of DFIG-based wind turbines,” *IEEE Trans.*, under review, 2022.

Implications: Hybrid Solar Inverter

FIDVR capability of hybrid PV power plants

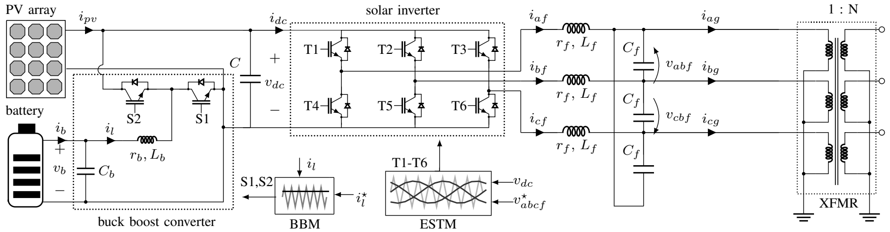

Implications: Mixed Power Systems

PSCAD: fault is applied at $t = 0\,$s and cleared at $t = 5/60\,$s

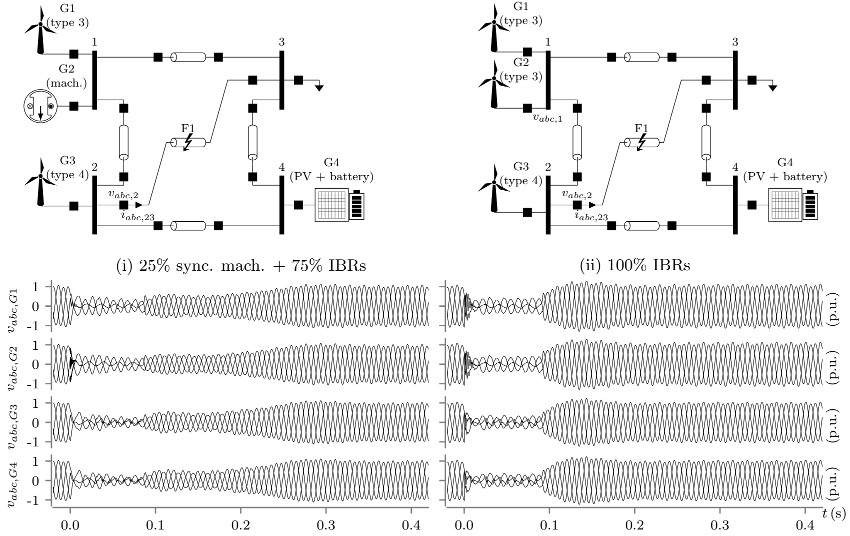

Thank You

- Demonstrated advances to grid-forming controls for restoration and fault ride-through capability of IBRs
- Set forth technology to engineer IBR-based grids that are resilient to blackouts and reliable to faults
- How to decide on the restoration actions of wind-dominant grids?